

A ~34 m.y. astronomical time scale for the uppermost Mississippian  
through Pennsylvanian of the Carboniferous System of the  
Paleo-Tethyan Realm

Huaichun Wu\*, Qiang Fang, Xiangdong Wang, Linda A. Hinnov, Yuping Qi,  
Shu-zhong Shen, Tianshui Yang, Haiyan Li, Jitao Chen, and Shihong Zhang

\*E-mail: whcgeo@cugb.edu.cn

**This Data Repository entry contains:**

1. Methods
2. Amplitude modulations of the astronomical parameters
3. Supplementary Figures DR1-DR7
4. Supplementary Tables DR1-DR3
5. Supplementary references cited

## 1. Methods

**Paleoclimatic and paleoenvironmental proxies.** All rock samples were crushed using a copper hammer, put into 8 cm<sup>3</sup> plastic boxes. Magnetic susceptibility (MS) was measured on a MFK1-FA Kappabridge before mass normalized. The anhysteretic remanent magnetization (ARM) of the 2.6 m – 15.6 m interval of the Naqing section was acquired by applying a peak alternating field of 0.1 T and a bias field of 50  $\mu$ T on the D-2000 AF demagnetizer, and the remanence intensity measurements were made on a JR6 spinner magnetometer. High-temperature-dependent susceptibility ( $\chi$ -T) was measured from room temperature to 700 °C in an argon atmosphere using a KLY-4S Kappabridge system with a CS-3 high-temperature apparatus (Fig. DR3). Low-temperature-dependent susceptibility ( $\chi$ -T) was measured from -200°C to room temperature. These measurements were conducted in the Paleomagnetism and Environmental Magnetism Laboratory at China University of Geosciences (Beijing). Magnetic hysteresis loops (Fig. DR3) were measured on representative samples at room temperature using a Vibrating Sample Magnetometer (Model VSM 3900, Princeton Measurements Corporation) at the Institute of Geology and Geophysics, Chinese Academy of Sciences.

Th is classically interpreted as reflecting clastic content in the carbonate succession (Da Silva et al., 2013). In order to assess possible detrital inputs and their influence on MS, Th data (~20 cm spacing) along 2.6 m-15.6 m of lower Naqing section was obtained using a RS-230 BGO Super-SPEC portable spectrometer.

**Pretreatment of the MS series for time series analysis.** In order to ensure that the minimum MS value in the Naqing exceeds zero to perform a logarithmic transformation, a formula of ( $y=x+5.5\times 10^{-9}$  m<sup>3</sup>/kg) was applied, where  $x$  is the MS value. The log<sub>10</sub>( $y$ ) transformation was carried out on the MS series in order to equalize the variance; the result is shown in **Figure 1**. The log-transformed MS series was pre-whitened before spectral analysis by removing a 10% weighted average for the combined Viséan-Serpukhovian, Bashkirian, and Moscovian, a 30% weighted

average for the Kasimovian, and a 15% weighted average for the combined Gzhelian and Visian-Gzhelian using Kaleidagraph (Cleveland, 1979).

**Amplitude modulation analysis.** The amplitude modulations of the interpreted astronomical signals were obtained using the power ratios of the variance of astronomical components to total variance. All modulation analyses are conducted in the software *Astrochron* (Meyers, 2014) in the "R" package (R Core Team, 2016).

## 2. Amplitude modulations of the astronomical parameters

Long period amplitude modulations of the orbital eccentricity can be isolated from the interfering terms  $\sim 95$  k.y. ( $g_4-g_5$ ) and  $\sim 99$  k.y. ( $g_3-g_5$ ), which are in-phase with two other short orbital eccentricity terms,  $\sim 124$  k.y. ( $g_4-g_2$ ) and  $\sim 130$  k.y. ( $g_3-g_2$ ). Long-period amplitude modulations of the obliquity variation can be isolated from the interfering terms  $\sim 41$  k.y. ( $p+s_3$ ) and  $\sim 39$  k.y. ( $p+s_4$ ), respectively. In these terms,  $s_3, s_4$  are the precession of nodes of the Earth and Mars, and  $g_2, g_3, g_4$  and  $g_5$  indicate the precession of perihelia of the Venus, Earth, Mars and Jupiter, and  $p$  is the Earth's axial precession frequency (Laskar et al., 2004). Thus, the long-period amplitude modulations in orbital eccentricity and obliquity correspond to  $g_4-g_3$  and  $s_4-s_3$ , respectively. The  $g_4-g_3$  and  $s_4-s_3$  terms indicate periods of 2.4 m.y. and 1.2 m.y., respectively, and reflect a secular resonance of  $(s_4-s_3)-2(g_4-g_3)=0$  from the present to  $\sim 40$  Ma (Laskar et al., 2004). However, prior to 40 Ma, the  $g_4-g_3$  and  $s_4-s_3$  terms are expected to have different periodicities due to chaotic resonance transitions between Earth and Mars (Laskar, 1990).

For the Carboniferous Period, the Naqing record indicates 136 and 96 k.y. periods for the short orbital eccentricity and a  $\sim 31$  k.y. period for the main obliquity term. We examined the long-period amplitude modulations of the observed orbital eccentricity and obliquity variations for evidence of secular resonance between Earth and Mars (Fig. DR7).

### 3. Supplementary Figures DR1-DR7

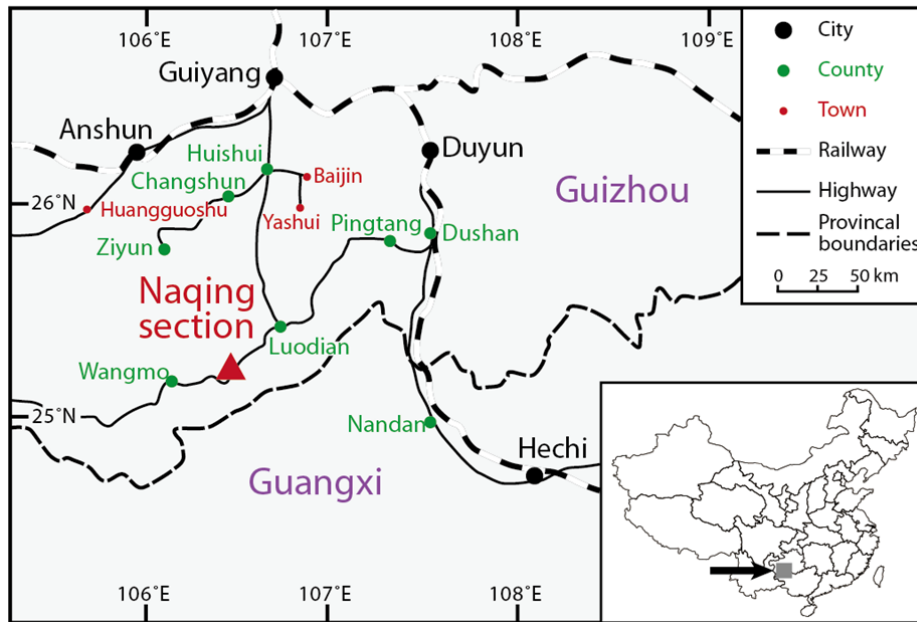
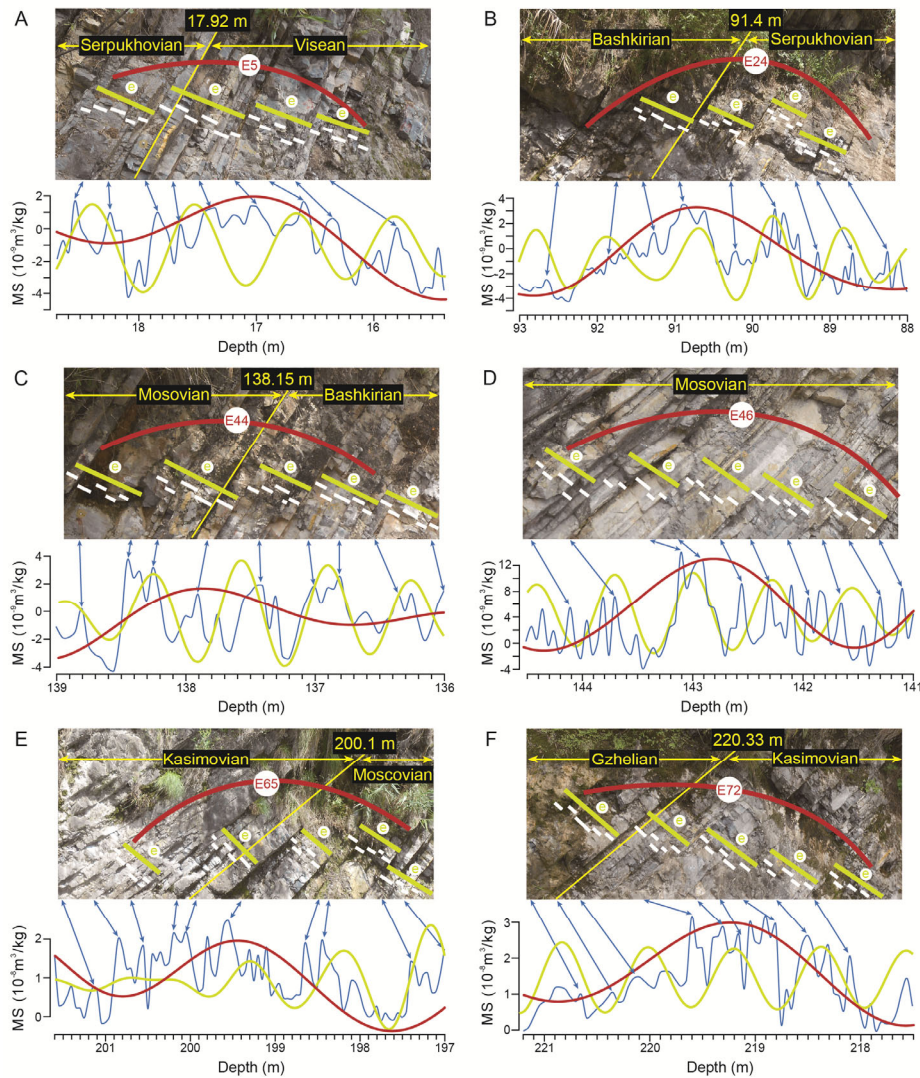
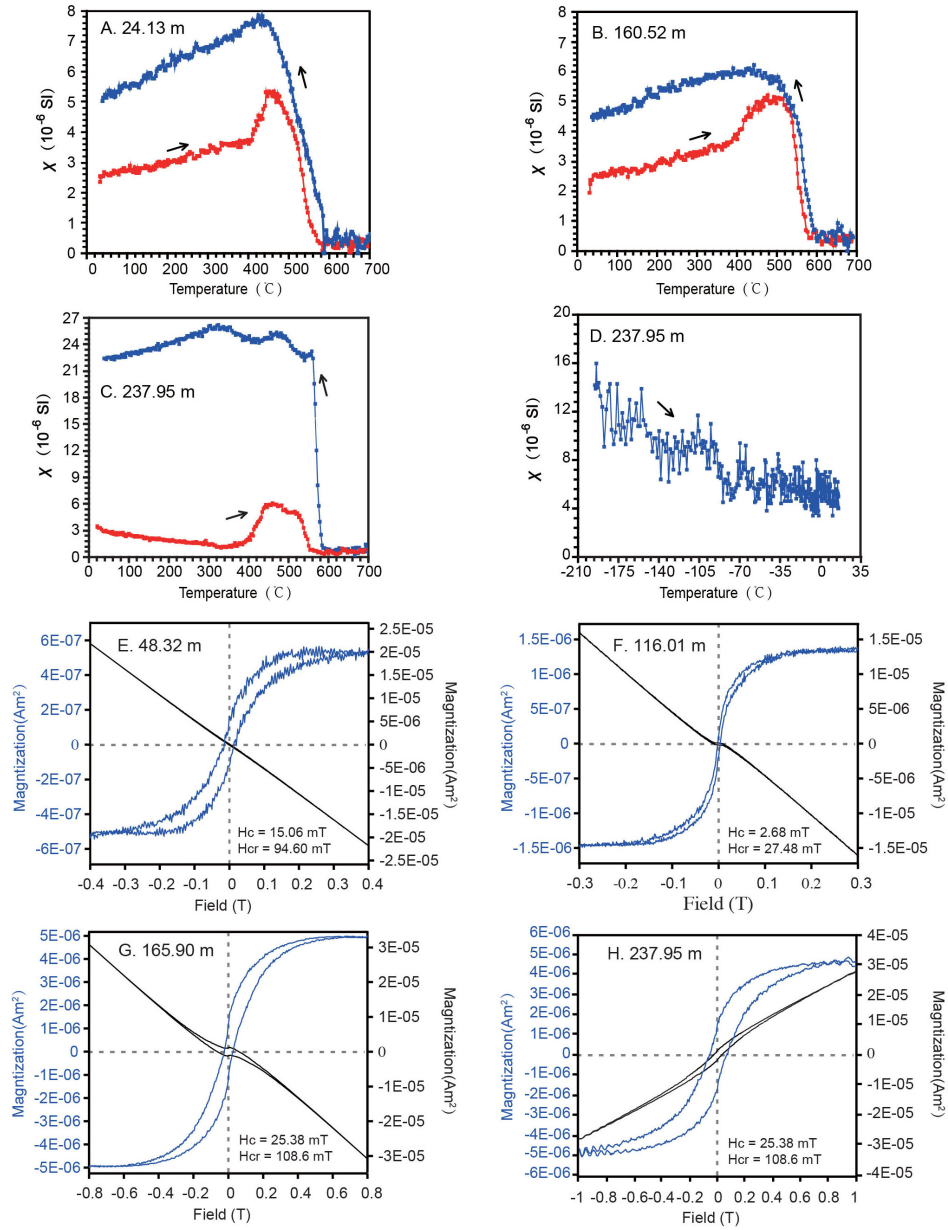


Figure DR1. Location map of the Naqing section of Luodian County, Guizhou province, China



**Figure DR2.** Relationship between magnetic susceptibility (MS) series and lithological cycles. Five thin precession-scale beds (white lines) are bundled into short orbital eccentricity cycles ("e", green lines), and four orbital eccentricity cycles are bundled into a long orbital eccentricity cycle ("E", red curve). The interpreted long orbital eccentricity curves are from Figure 1. The short orbital eccentricity curves were Gaussian band-pass filtered from MS series with frequencies of  $1.13 \pm 0.2$  cycles/m for A and B,  $1.49 \pm 0.2$  cycles/m for C and D,  $1.1 \pm 0.2$  cycles/m for E and F, respectively.



**Figure DR3.** (A-D) Typical low-field susceptibility curves versus temperature for representative samples. The red and blue lines indicate heating and cooling curves, respectively. (E-H) Diagrams of room temperature hysteresis loops for representative rock samples. The black and blue lines represent before and after paramagnetic slope correction results.

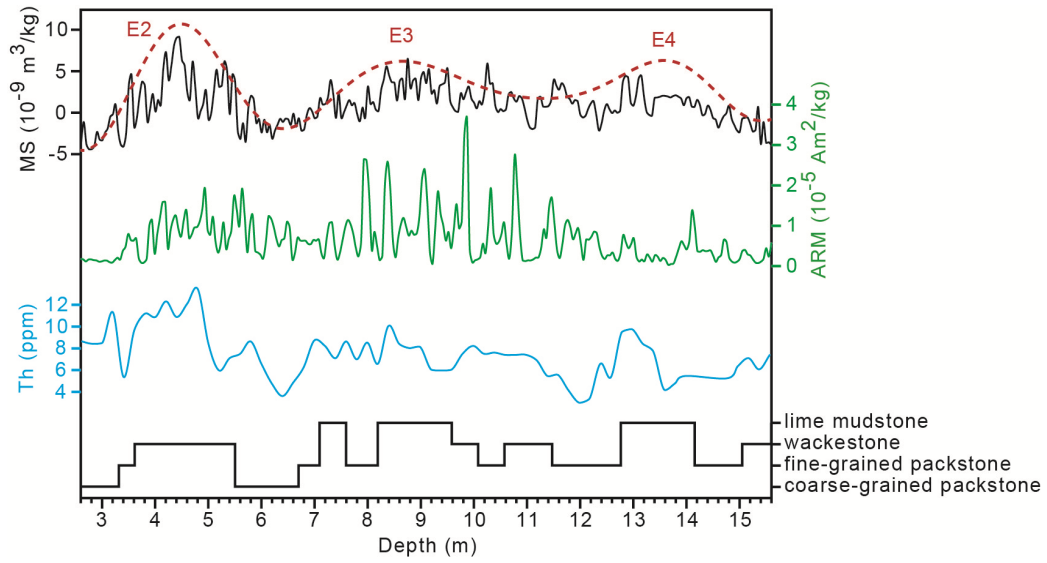


**Figure DR4.** Comparison of magnetic susceptibility (MS), anhysteretic remanent magnetization (ARM), Th content and lithology from lower Naqing section. The red dashed curve is 405 k.y. long eccentricity filtering output from Fig. 1.

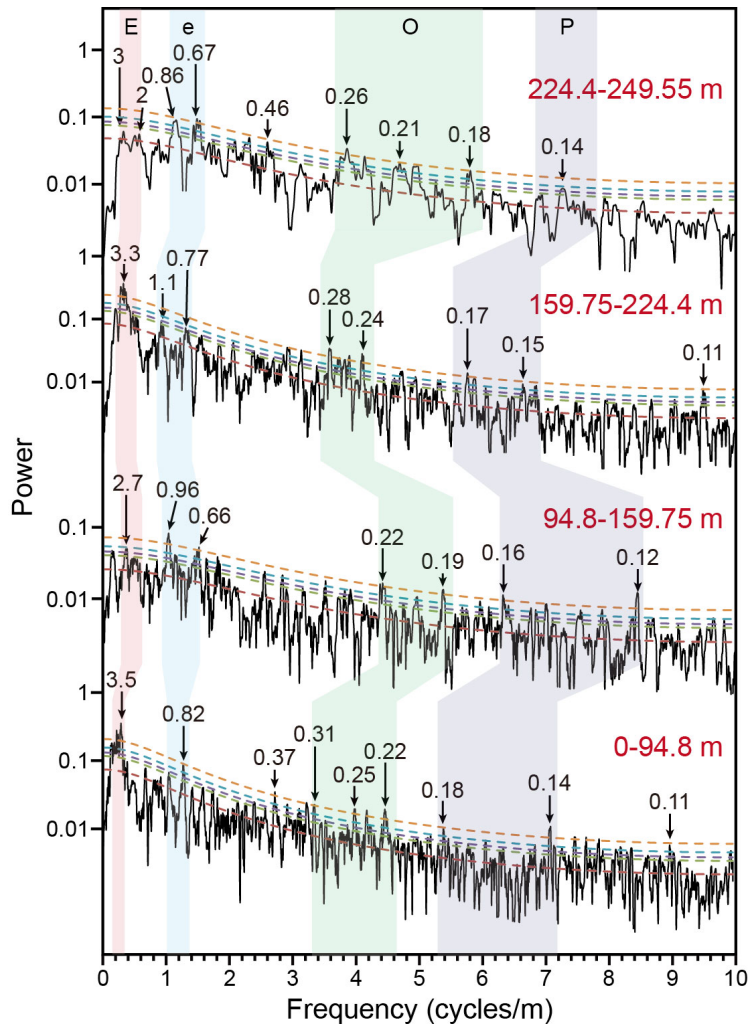


**Figure DR5.**  $2\pi$  MTM power spectra of the MS series subsets. Significant peaks are labeled in meters. The red, green, purple, blue and orange dashed curves represent the classical red noise spectrum model of the series, with 50%, 85%, 90%, and 95% confidence levels.

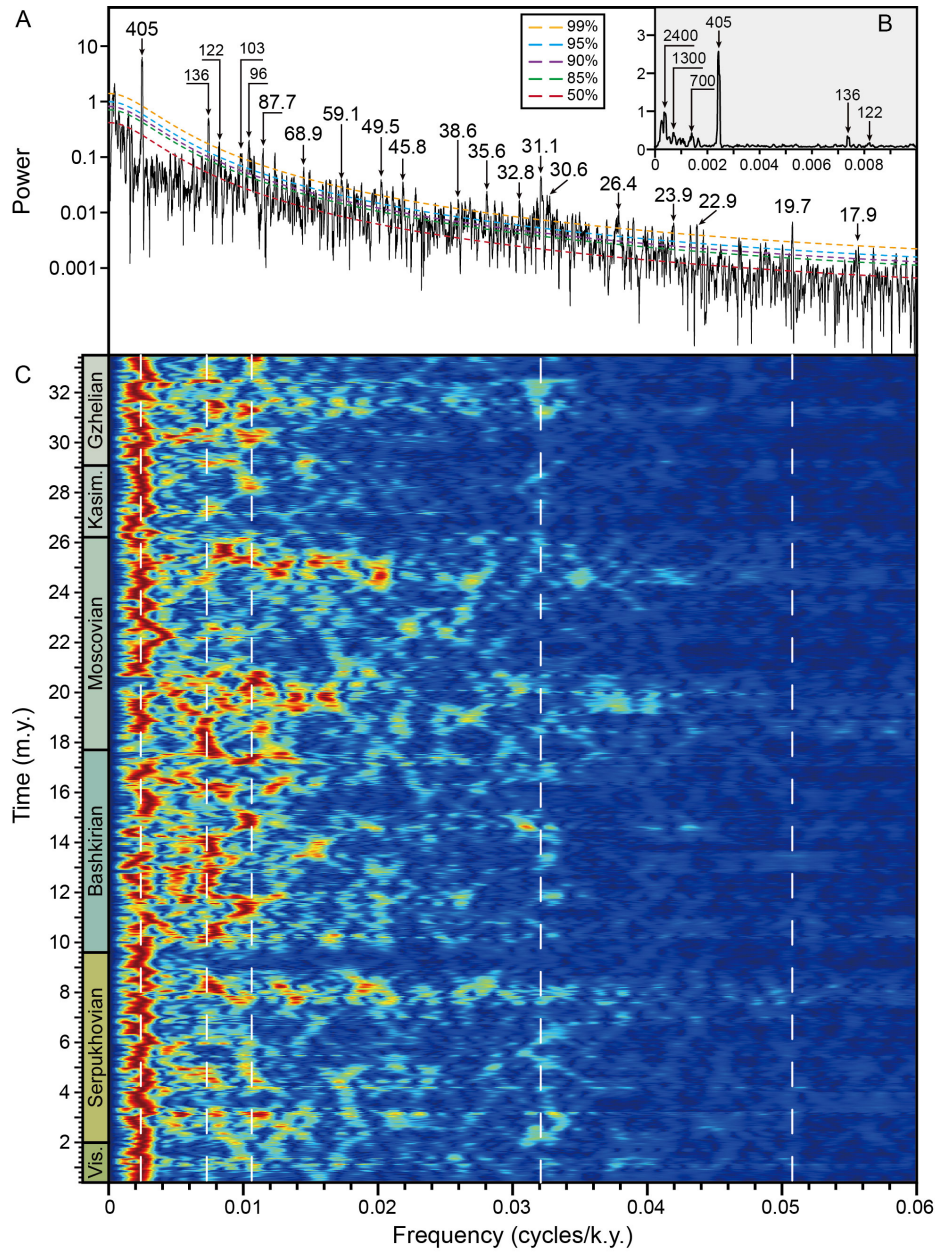


**Figure DR6.** Spectral analysis of the 405 k.y. calibrated MS time series at Naqing. A:  $2\pi$  MTM power spectrum of the MS time series after subtracting a 10% weighted average. B:  $2\pi$  MTM power spectrum of the calibrated MS series after subtracting a 20% weighted average to show the low-frequency portion of the spectrum. C: Evolutionary fast Fourier transform spectrogram with an 800 k.y. sliding window and 5 k.y. step.

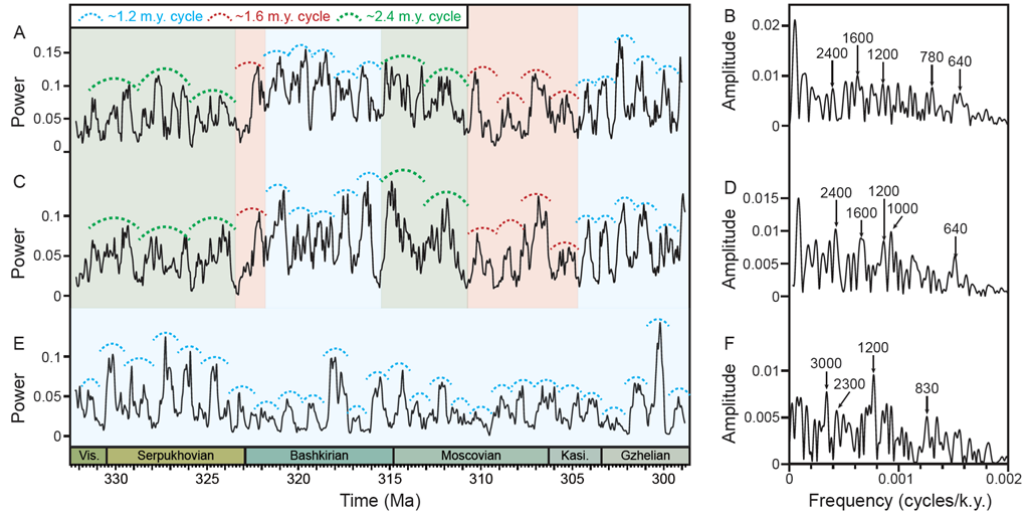


**Figure DR7.** The ratios of astronomical signal variance to total variance and their amplitude spectra. 136 k.y. short orbital eccentricity variance ratio (A), 96 k.y. short orbital eccentricity variance ratio (C) and 31 k.y. obliquity variance ratio (E) was with cutoff frequencies were 0.007 and 0.0085 cycles/k.y., 0.0096 and 0.011 cycles/k.y., and 0.03 and 0.034 cycles/k.y. from time-calibrated MS series, respectively.  $2\pi$  MTM amplitude spectra of (A), (C) and (E) were computed with Analyseries, and are shown in (B), (D) and (F), respectively.

## 4. Supplementary Tables DR1-DR3

**Table DR1.** Astronomically estimated durations of stages and conodont zones at Naqing and numerical durations from GTS2012 (Davydov et al., 2012) and GTS2016 (Ogg et al., 2016) for comparison. The depth has been calibrated to the aluminum pin scale provided by the working group from the International Commission on Stratigraphy, Subcommittee on Carboniferous Stratigraphy.

Stage	Conodont zone	Depth (m)	Duration (k.y.)		
			This study	GTS2012	GTS2016
<b>Gzhelian</b>		<b>220.33–249.52</b>	<b>4831.6</b>	<b>4800</b>	<b>4500</b>
	<i>Streptognathodus wabaunsensis</i>	242.68–249.52	1022.7	-	-
	<i>Streptognathodus tenuialveus</i>	232.29–242.68	1844.2	-	-
	<i>Streptognathodus virgilicus</i>	227.95–232.29	668.3	1000	2400
	<i>Idiognathodus nashuiensis</i>	221.81–227.95	1103.6	-	-
	<i>Idiognathodus simulator</i>	220.33–221.81	192.9	800	400
<b>Kasimovian</b>		<b>200.1–220.33</b>	<b>2869.1</b>	<b>3300</b>	<b>3300</b>
	<i>Streptognathodus zethus</i>	212.74–220.33	958.9	-	-
	<i>Idiognathodus eudoraensis</i>	212.09–212.74	82.3	-	-
	<i>Idiognathodus guizhouensis</i>	207.46–212.09	707.4	-	-
	<i>Idiognathodus magnificus</i>	202.67–207.46	780.8	-	-
	<i>Idiognathodus turbatus</i>	200.1–202.67	339.8	-	-
<b>Moscovian</b>		<b>138.15–200.1</b>	<b>8499</b>	<b>8200</b>	<b>7900</b>
	<i>Swadelina makhlinae</i>	190.36–200.1	1252.6	-	-
	<i>Swadelina subexcelsa</i>	176.78–190.36	1566.4	-	-
	<i>Idiognathodus podolskensis</i>	157.01–176.78	2781.2	-	2800
	<i>Mesogondolella donbassica-</i>	142.41–157.01	2259.4	-	-
	<i>Mesogondolella clarki</i>				
	<i>Diplognathodus ellesmerensis</i>	138.15–142.41	639.4	-	-
<b>Bashkirian</b>		<b>91.4–138.15</b>	<b>8097.6</b>	<b>8000</b>	<b>8600</b>
	“ <i>Streptognathodus</i> ” <i>expansus</i> M2	131.19–138.15	1455.3	-	-
	“ <i>Streptognathodus</i> ” <i>expansus</i> M1	122.94–131.19	1671	-	-
	<i>Idiognathodus primulus</i>	120.47–122.94	349.7	-	-
	<i>Neognathodus symmetricus</i>	117.7–120.47	429.1	-	-
	<i>Idiognathoides sinuatus</i>	105.49–117.7	2320.3	1700	1700
	<i>Declinognathodus noduliferus</i>	91.4–105.49	1872.2	700	700
<b>Serpukhovian</b>		<b>17.92–91.4</b>	<b>7598</b>	<b>7700</b>	<b>7700</b>
	<i>Gnathodus bilineatus bollandensis</i>	58.47–91.4	2993.4	1800	1800
	<i>Lochriea zieglerei</i>	17.92–58.47	4604.6	1400	1400
<b>Visean</b>			<b>2004.8</b>	<b>15800</b>	
	<i>Lochriea nodosa</i>	7.42–17.92	1097.4	1100	-
	<i>Gnathodus bilineatus bilineatus</i>	0–7.42	907.4		

**Table DR2.** Magnetic susceptibility data in depth and astronomical tuned age for the Naqing section (in a separate supplementary data file): 2019036\_Table DR2.xlsx.

**Table DR3.** Frequency ratios of astronomical periodicities for the Devonian/Carboniferous boundary (358.9 Ma), basal Serpukhovian Stage (330.9 Ma), middle Carboniferous (323.2 Ma) and Carboniferous/Permian boundary (298.9 Ma). The periods of long and short eccentricity are from [Hinnov \(2000\)](#). Three sets of obliquity and precession periods were obtained using linear interpolation from the data of 298 Ma and 380 Ma ([Berger and Loutre, 1994](#)), extrapolation with equations (Yao et al., 2015) based on La2004 model (Laskar et al., 2004), and the Milankovitch Calculator <https://davidwaltham.com/wp-content/uploads/2014/01/Milankovitch.html> ([Waltham, 2015](#)).

Calculated period of orbital parameters using model of Berger and Loutre (1994) / Laskar et al. (2004) / Waltham (2015) in k.y.							Ratio	Age (Ma)
E	e2	e1	O1	P1	P2			
405	128	95	34.14/	20.67/	17.38/	23.3: 7.36: 5.47: 1.96: 1.19: 1	298.9	
				31.08/	19.2/	16.82/		24.08: 7.61: 5.65: 1.85: 1.14: 1/
				35.5	21.7	17.67		22:92: 7.24: 5.38: 2.01: 1.23: 1
405	128	95	33.62/	20.47/	17.24/	23.49: 7.42: 5.51: 1.95: 1.19: 1/	323.2	
				30.27/	18.94/	16.63/		24.35: 7.7: 5.71: 1.82: 1.14: 1/
				35.1	21.6	17.57		23.05: 7.29: 5.41: 2: 1.23: 1
405	128	95	33.45/	20.41/	17.2/	23.55: 7.44: 5.52: 1.94: 1.12: 1/	330.9	
				30.01/	18.87/	16.57/		24.44: 7.72: 5.73: 1.81: 1.14: 1/
				35	21.5	17.54		23.1: 7.3: 5.42: 2: 1.23: 1
405	128	95	32.85/	20.19/	17.04/	23.77: 7.51: 5.58: 1.93: 1.18: 1/	358.9	
				29.52/	18.55/	16.34/		24.79: 7.83: 5.81: 1.8: 1.14: 1/
				34.6	21.4	17.42		23.25: 7.35: 5.45: 1.99: 1.23: 1

## 5. Supplementary references cited

- Berger, A., and Loutre, M.F., 1994, Astronomical forcing through geological time, in De Boer, P.L., and Smith, D.G., eds., *Orbital forcing and cyclic sequences*, Volume 19: Oxford, Blackwell Scientific Publications, p. 15–24, doi:10.1002/9781444304039.ch2.
- Cleveland, W.S., 1979. Robust locally weighted regression and smoothing scatterplots. *J. Am. Stat. Assoc.*, v. 74, p. 829–836.
- Davydov, V.I., Korn, D., and Schmitz, M.D., 2012. The Carboniferous Period. In: Gradstein, F.M., Ogg, J.G., Schmitz, M., Ogg, G. (Eds.), *The Geologic Time Scale 2012*. Elsevier, pp. 602–651.
- Hinnov, L. A., 2000, New Perspectives on Orbitally Forced Stratigraphy: *Annual Review of Earth and Planetary Sciences*, v. 28, no. 1, p. 419–475, doi:10.1146/annurev.earth.28.1.419.
- Laskar, J., 1990, The chaotic motion of the solar system: A numerical estimate of the size of the chaotic zones: *Icarus*, v. 88, no. 2, p. 266–291, doi:10.1016/0019-1035(90)90084-M.
- Laskar, J., Joutel, F., and Boudin, F., 1993, Orbital, precessional, and insolation quantities for the earth from -20 Myr to +10 Myr: *Astronomy & Astrophysics*, v. 270, no. 1–2, p. 522–533.
- Laskar, J., Robutel, P., Joutel, F., Gastineau, M., Correia, A. C. M., and Levrard, B., 2004, A long-term numerical solution for the insolation quantities of the Earth: *Astronomy & Astrophysics*, v. 428, no. 1, p. 261–285, doi:10.1051/0004-6361:20041335.
- Meyers, S.R., 2014, *Astrochron: An R Package for Astrochronology*. Version 0.3.1.
- Ogg, J., Ogg, G., and Gradstein, F., 2016, *A Concise Geologic Time Scale 2016*, 234 p., doi: 10.1016/B978-0-444-59467-9.00001-7.
- R Core Team. *R: A Language and Environment for Statistical Computing*, 2016, R Foundation for Statistical Computing, <http://www.R-project.org/>.

Waltham, D., 2015, Milankovitch period uncertainties and their impact on cyclostratigraphy: *Journal of Sedimentary Research*, v. 85, no. 8, p. 990–998, doi:10.2110/jsr.2015.66.

Yao, X., Zhou, Y. Q., and Hinnov, L. A., 2015, Astronomical forcing of a Middle Permian chert sequence in Chaohu, South China: *Earth and Planetary Science Letters*, v. 422, p. 206–221.